Available online at www.sciencedirect.com

ScienceDirect

journal homepage: www.elsevier.com/locate/he

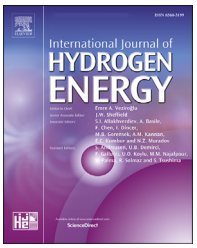

Hydrogen addition to a commercial self-aspirating burner and assessment of a practical burner modification strategy to improve performance

Adam J. Gee [a,*], *Douglas B. Proud* [a], *Neil Smith* [b], *Alfonso Chinnici* [a], *Paul R. Medwell* [a]

[a] School of Electrical and Mechanical Engineering, The University of Adelaide, Adelaide, SA 5005, Australia
[b] School of Chemical Engineering and Advanced Materials, The University of Adelaide, Adelaide, SA 5005, Australia

HIGHLIGHTS

- Flashback limit of a self-aspirating burner extended up to 100 vol% H_2 by increasing d_{jet}.
- Primary air entrainment is reduced by increasing d_{jet}.
- Positive non-linear relationship between equivalence ratio and flame length.
- Negligible reductions in radiant heat transfer with H_2 addition under in modified burner.
- Negative linear relationship between NOx emissions and equivalence ratio.

ARTICLE INFO

Article history:
Received 10 April 2023
Received in revised form
19 June 2023
Accepted 20 June 2023
Available online xxx

Keywords:
Commercial
Burner
Hydrogen
Fuels
NOx

ABSTRACT

The ability for existing burners to operate safely and efficiently on hydrogen-blended fuels is a primary concern for the many industries looking to adopt hydrogen as an alternative fuel. This study investigates the efficacy of increasing fuel injector diameter as a simple modification strategy to extend the hydrogen-blending limits before flashback. The collateral effects of this modification are quantified with respect to a set of key performance criteria. The results show that the unmodified burner can sustain up to 50 vol% hydrogen addition before flashback. Increasing the fuel injector diameter reduces primary aeration, allowing for stable operation on up to 100% hydrogen. The flame length, visibility and radiant heat transfer properties are all increased as a result of the reduced air entrainment with a trade-off reported for NOx emissions, where, in addition to the effects of hydrogen, reducing air entrainment further increases NOx emissions.

Introduction

Due to the current state of climate change, there is a need to consider the effects of hydrogen (H_2) as an alternative fuel to natural gas in domestic and industrial combustion applications. The potential benefits from adoption of hydrogen are well-documented, in particular, a renewable and ethical production process, carbon-free emissions and improved performance. For the many high temperature commercial

* *Corresponding author.*
E-mail address: adam.gee@adelaide.edu.au (A.J. Gee).

https://doi.org/10.1016/j.ijhydene.2023.06.230

Nomenclature

ρ	density
U	velocity
A	area
R	radius
$\dot{V}$	volumetric flow rate
$\dot{m}$	mass flow rate
φ	equivalence ratio
HHV	higher heating value
LHV	lower heating value
χ_r	radiant fraction
Q_t	total heat input
Q_r	total radiated power
x	mole fraction of methane
SLPM	standard litres per minute
EI	emission index
D_f	dilution correction factor
MW	molecular weight
PCC	Pearson correlation coefficient
HAB	height above burner
Ψ	ratio of entrained air to fuel flow
Re	Reynolds number

applications looking to utilize renewable, low-carbon technology which are not well suited for electrification, hydrogen combustion is a promising alternative [1].

Despite the advantages, adding hydrogen to natural gas burners changes the combustion characteristics around which the burners were designed [2–4]. Hydrogen has a higher laminar burning velocity and adiabatic flame temperature, which increases the potential for flashback and thermal NOx production. The lack of carbon in hydrogen also poses a challenge of reduced radiant heat transfer and visibility — the radiant heat and much of the visible emissions from typical hydrocarbon flames are primarily a result of carbonaceous soot particles [3,5–9]. Much of the recent investigations of hydrogen combustion has been focused on solving these challenges via alternative combustion regimes [10], fuel additives [11–13] and various modifications to burner design [14]. The effects of blending with hydrogen vary depending on the fuel type, performance metrics and fraction of total fuel. The consensus is most natural gas burners can tolerate around 10 vol% hydrogen before any impact on performance is observed, although higher tolerances have also been reported [1,12,15–19]. Although the 10 vol% mark serves as a good initial target for early adopters of hydrogen, it will not be sufficient in the long term to reduce carbon emissions and limit our dependence on non-renewable fuels. The long-term goals of governments and industries looking to transition to hydrogen will need to achieve higher blend ratios closer to 100 vol% to have an impact on carbon emissions.

The focus of future burner design needs to address the challenges of hydrogen adoption on industry-applicable burners for blending scenarios beyond 10–20% and where possible, propose strategies to smoothly integrate hydrogen as a primary fuel for combustion. Hydrogen research is rarely conducted on commercial burners due to the additional scale and complexity of their design, which is not intended for fundamental-level study. Studying small scale burners with simple designs is useful for detailed analysis of underlying chemistry and physics but this approach does not provide a global context of the effects of an alternative fuel. In particular, when studying hydrogen addition in self-aspirating burners it can be difficult to quantify important parameters such entrained air, which is critical to describe the premixing behaviour [16]. The subtle complexities of practical commercial burners make predicting the outcomes of alternative fuel use difficult. Modern self-aspirating burners often include unique and bespoke design features that require targeted investigations to bridge the knowledge gap on the effects of hydrogen addition and inform manufacturers, end-users and policy makers of the benefits and challenges involved in a transition to hydrogen.

Self-aspirating burners are commonly used in a wide range of applications, from small Bunsen burners and domestic cooktops, up to medium and larger scale burners used in commercial kitchens and metal processing. The principle of operation of these types of burners has been known for many years [20,21]. A fuel gas mixture exiting an injector with enough momentum to entrain atmospheric air, creating a partially-premixed fuel-air mixture [20–22]. The amount of entrained air is a function of fuel momentum (ρU^2), therefore, factors such as burner geometry, fuel type and fuel pressure are important dictating parameters of the fuel/air mixture and overall performance [23,24]. This sensitivity to multiple factors means that a subtle variation in experimental methods can yield conflicting results between similar investigations.

The operating limits of self-aspirating burners on hydrogen has become a notable area of interest in recent years. This new motivation for studying hydrogen in self-aspirating burners has highlighted the challenges in predicting the safe upper limit for hydrogen addition to existing domestic and commercial burners. In principle, flashback occurs when the burning velocity of a fuel exceeds the gas velocity at which it is being issued [25–27]. In practice, flashback can occur as a result of instabilities in temperature, pressure, flame propagation dynamics or a number of other factors. The critical flashback limit of a given burner or fuel needs to be described with some degree of insight to the operating conditions. For example, the flashback limit of a burner during ignition may not be the same as the limit during steady state operation. As the system approaches the flashback limit, fluctuations in the temperature of inlet gases or burner components, fuel/air flow or changes in the supply/turndown rate may trigger a flashback event. The reported upper limit for hydrogen addition to any given burner is often inconsistent due to the sensitivity of flashback to steady or unsteady operating conditions, confined or unconfined combustion and other subtle variations in the design and testing methodology. Zhao et al. [17,18,28,29] has contributed a large body of work on the topic of flashback in self-aspirating burners due to hydrogen addition. In an investigation on hydrogen addition to a 22 kW self-aspirating furnace room heater, the burner would flashback during ignition at 20% but could sustain up to 45% hydrogen during steady-state operation [30]. A similar investigation of a self-aspirating cooktop burner found the limit of hydrogen

Please cite this article as: Gee AJ et al., Hydrogen addition to a commercial self-aspirating burner and assessment of a practical burner modification strategy to improve performance, International Journal of Hydrogen Energy, https://doi.org/10.1016/j.ijhydene.2023.06.230

addition before flashback to be 75% during steady-state operating conditions but this value is reduced to 20% when the ignition/turn-down capacities of the burner are included in the test [17]. In the same study, intermittent flashback limits were discovered by changing operating conditions slightly, such as, for example, the use of a cooking pot. Interactions between the pot surface and the flame caused the steady-state hydrogen limit before flashback to be reduced to 55%. Other investigations also concluded that the upper limit for hydrogen addition before flashback during ignition or similar was 10–30% [1,15,18,29,31–33]. It is noteworthy, however, that this limit can be significantly extended with simple modifications to the burner or the operating procedure, such as, for example, increasing the hydrogen fraction under steady state conditions [17,29].

The efficacy of a burner modification strategy to extend the hydrogen blending limit must also be weighed against its impact on other key performance parameters. Flame length, visibility, radiant heat transfer and NOx emissions are commonly cited areas of concern when considering hydrogen blending [34–37]. Many commercial burners utilize the self-aspirating design to entrain cool primary air to provide a critical cooling effect to the burner components. In an investigation on the effects of hydrogen addition to a self-aspirating water heater, it was reported that 40% hydrogen could be blended with natural gas before the burner surface temperature exceeded safe limits [38]. The adiabatic flame temperature of hydrogen is much higher than other fuels, including natural gas. The increased flame temperature may pose added risk to the burner equipment. However, flame temperatures also depend on stoichiometry, which is a function of burner design and operation, and temperatures of burner components depend on heat transfer, which also depends on design and operation. These factors also impact the formation of thermally sensitive species such as NOx. The potential increased flame temperature as a result of hydrogen addition is frequently correlated with increased thermal NOx formation. For counterflow partially-premixed flames in internal combustion engines, numerical simulations have shown that the extent of partial premixing (equivalence ratio) and strain rate both have an effect on NOx emissions, and that the prompt NOx mechanism can dominate over the thermal mechanism [39]. For inverse diffusion flames it has been noted that hydrogen blending can slightly increase NOx emissions [40]. It is interesting to note that the impact of hydrogen on NOx emissions is frequently reported as negligible in self-aspirating burners for 20–25 vol% [18,28], 40–50 vol% [17,38,41] and even up to 80 vol% [42]. The impact of hydrogen addition >50 vol% is rarely investigated for commercial self-aspirating burners due to the risk of flashback.

In addition to increased flashback potential and NOx emissions, hydrogen-blended flames have also been reported to impact heat transfer efficiencies [36,43–47]. The zero carbon-dioxide emission profile is a flagship feature of hydrogen as an alternative fuel compared to natural gas and other hydrocarbon fuels. Given the absence of carbon-species in hydrogen, a partial or complete replacement of carbon-based fuels for hydrogen will play a significant role in reducing carbon emissions in industries which choose to adopt hydrogen. However, although counterintuitive, the presence of carbon is a critical component to the heat transfer properties of a flame. Soot particles are responsible for the majority of the radiant heat transfer in hydrocarbon flames. Their presence is critical to the thermal efficiency of numerous commercial heating applications that rely on radiation in addition to convection heat transfer. Other species such as water vapour do contribute to radiant heat transfer but are not as efficient emitters as soot particles. The reduced radiant heat transfer of hydrogen flames has been previously correlated with a reduced soot volume fraction due to displaced carbon in the fuel.

The impact of hydrogen blending on the flashback limits and performance of commercial self-aspirating burners, and in particular, the Atmospheric Nozzle or "AN" burner, is not sufficiently addressed in the current literature. Similarly, an analysis of the efficacy and collateral effects of the modification of fuel injector size to extend the flashback limit has not been adequately investigated. The differences in the burner structure and operating conditions in previous studies, have resulted in a divided consensus on the safe upper limit for hydrogen blending in commercial applications. Classification of equipment failure can be highly subjective across industries and policy guidelines. The changes in equipment surface temperature, heat transfer efficiencies or emission of some combustion species due to hydrogen addition may be acceptable to some but intolerable to others. Much of the contemporary research concludes that current self-aspirating burners have varying tolerances to hydrogen but in general 20% hydrogen can be added without flashback or other any negative consequences. There is evidence to suggest that the potential for flashback can be reduced via simple modification to the burner geometry, in particular, the fuel injector size [29]. More work and data are needed to establish the efficacy of such burner modifications and their collateral effects on performance.

The aims of the present investigation are to quantify the effects of hydrogen addition to a commercially available, self-aspirating, atmospheric nozzle burner, commonly referred to as an AN-burner. The AN-burner and its design features are commonly used in a wide range of domestic and industrial applications, many of which are potential adopters of hydrogen in the future. The first aim is to quantify the effects of various hydrogen/natural gas fuel blends under normal operating conditions. The primary air entrainment is measured for each hydrogen/natural gas fuel blend and the upper limit of hydrogen addition before flashback is determined. The second aim is to establish the effectiveness of a simple modification of the fuel injector to extend the hydrogen blending limit before flashback. Finally, in addition to the impact of hydrogen addition, the collateral effects of this modification strategy are assessed with respect to several key performance criteria, namely, flashback resistance, flame visibility/appearance, radiant heat transfer and flue gas NOx emissions. The knowledge generated from these results will provide new understanding of (i) the impact of hydrogen use in existing gas appliances at various blend ratios and (ii) the efficacy and collateral effects of a simple, low-cost and retrospective modification strategy to

Please cite this article as: Gee AJ et al., Hydrogen addition to a commercial self-aspirating burner and assessment of a practical burner modification strategy to improve performance, International Journal of Hydrogen Energy, https://doi.org/10.1016/j.ijhydene.2023.06.230

extend hydrogen blending limits. The novel experimental data generated from this work will contribute to de-risking the adoption of hydrogen by providing insight into the manner and magnitude by which hydrogen-blending affects burner performance. Overall, this work will build on discussion on the merit of hydrogen as an alternative fuel in existing burner infrastructure and provide a basis for future work to investigate implementation strategies for hydrogen.

Methods

Burner apparatus

Partially-premixed flames are common in domestic and commercial applications because of their combination of soot-free combustion, utility, and safety. A rich premixed blend of fuel and air helps to reduce soot and carbon monoxide levels, while maintaining flame stability. In practice, partially-premixed flames are most commonly achieved using a self-aspirating design.

Self-aspirating burners operate by utilising fuel stream momentum to entrain primary air from the surrounding atmosphere into a mixing tube upstream of the burner exit. The rich fuel/air mixture is ignited at the burner exit where secondary air sustains the reaction. The rate of entrained primary air is a function of fuel momentum and so factors related to fuel properties or burner geometry can have a strong influence on the entrainment potential of the burner and the stoichiometry of the resulting mixture [22]. Practical self-aspirating burners have geometric features such as fuel injector diameter based on fuel properties and required power output of the burner to ensure a high level of flame stability and good combustion efficiency. Momentum flux (ρU^2) is most commonly used in gas-entrainment applications [23,24], however, since the geometry (area) is not a fixed variable in this investigation, a momentum flow ($\rho U^2 A$) term is also used.

The burner apparatus used in these experiments was a 35 kW, commercially available, self-aspirating, natural gas burner with an atmospheric nozzle. A diagram of the burner apparatus is presented in Fig. 1. Fuel was issued into the base of the burner tube via a 4 mm diameter fuel injector (d_{jet}). Primary air was entrained from the surroundings into a 68.5 mm diameter venturi inlet from where it was allowed to mix in the 112.5 mm burner tube with the fuel before exiting the burner head. Surrounding air in entrained radially through the two open-walled sections of the venturi inlet. The primary air inlet also features an adjustable valve at the venturi to control the primary aeration. For this investigation, the valve was kept completely open to maximise air intake, which is a common operating state of the AN-burner.

Standard operation of the AN-burner uses a pressure regulator to control the supply rate of natural gas with primary air naturally entrained by the momentum of the fuel. However, in this investigation, the pressure regulators were removed from the burner apparatus and the mass flow rate of hydrogen and natural gas was controlled manually using individual mass flow controllers. The use of mass flow controllers allows for precise control of individual fuel flow rates

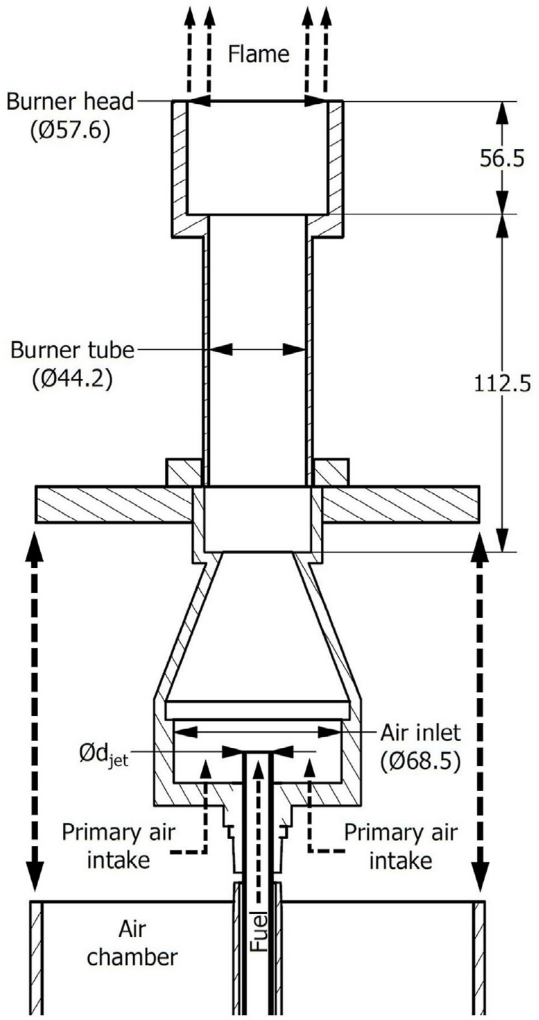

Fig. 1 – Diagram of AN-burner showing major components and their sizes in millimetres. Fuel injector jet diameter(s) is interchangeable as d_{jet} = 4 mm, 8 mm or 12 mm. Fuel is issued via the central jet with diameter d_{jet} and air is entrained radially from the surroundings via the open-walled design of the venturi inlet. The air chamber is shown in the open position (slid down to allow normal atmospheric air entrainment) but can be raised and sealed to the mounting flange to measure and control the air supply.

to conserve the heat input of the base natural gas case at various hydrogen-natural gas blend ratios. This approach allowed for an analysis of the upper hydrogen limit before flashback under steady state operating conditions. The entrainment of primary air was also measured using mass flow controllers. A known mass flow rate of air was fed through diffusers to a sealed chamber around the air intake of the burner. A manometer was used to create an open control-loop to ensure atmospheric pressure was maintained inside the chamber during operation. This approach, adapted from previous work, enables the quantification and control of the mass flow of air for the burner when operating on different fuel blends [48]. This measured primary air is also compared with theoretical values which have been generated using a

Please cite this article as: Gee AJ et al., Hydrogen addition to a commercial self-aspirating burner and assessment of a practical burner modification strategy to improve performance, International Journal of Hydrogen Energy, https://doi.org/10.1016/j.ijhydene.2023.06.230

predictive model from literature [18,22]. The model, presented in Eq. (1), is a function of fuel density (ρ_{fuel}), air density (ρ_{air}), inner (fuel) tube area (A_1) and outer annulus (air) area (A_2) to determine a ratio (Ψ), of entrained air to fuel supply. In this case, A_1 is calculated using d_{jet} and A_2 is calculated using the venturi air inlet diameter (68.5 mm), as shown in Fig. 1. The agreement between measured experimental data and the theoretical calculation is discussed further in Section 3.1, in addition to the influence of changes in density and fuel stream velocity caused by hydrogen addition.

$$\Psi = \sqrt{\frac{\rho_{fuel}}{\rho_{air}}}\left(\sqrt{\frac{A_2}{A_1}} - 1\right) \quad (1)$$

The addition of hydrogen changes the equivalence ratio of the fuel blend due to its own unique stoichiometry and its increased propensity for air entrainment when blended at constant heat input. The impact of hydrogen addition may be mitigated using this insight by modifying the fuel injector size. Increasing fuel injector diameter is a simple approach that can be made retrospectively to existing burner systems. Increased fuel injector size will lower jet velocity and decrease the entrained air. The resulting equivalence ratio will be richer and may allow for increased hydrogen blending before flashback. In order to study how changes in fuel composition and consequently, momentum, affects the performance of the burner, the fuel jet diameter is increased from the stock 4 mm, up to 8 mm and 12 mm. Note that the same effect could also be achieved by setting the venturi valve such that the same amount of air is entrained — however, manipulating the venturi valve is less precise and more difficult to repeat than replacing the fuel injector. Unless otherwise specified, all data, including flashback limits are reported at full rate (35 kW) for operation at steady state conditions.

Flame cases

Typical operation of the AN-burner consists of natural gas supplied at 35 kW through a 4 mm fuel injector at 1–2 kPa. The heat input from the fuel stream is held constant at 35 kW and is achieved by adjusting the fuel supply pressure, albeit indirectly through the electronic mass flow controllers. The motivation for the work is understanding the role of hydrogen addition on combustion performance, and it is assumed the heat requirements for a future application would be constant. Pressure regulator settings may need to be adjusted in practical retrofitting applications when using hydrogen. A topic for future work in this area is to investigate the modification of a burner which can operate at 100 vol% hydrogen and constant inlet pressure. For indicative purposes, Fig. S3 in the Supplementary Material reports calculated pressure values for the various jet diameter cases presented in this work.

The most common air setting is for the venturi valve to be kept completely open, allowing maximum air entrainment. The natural gas used in these experiments was from the municipal network, with an approximate composition provided in Table S1 of the Supplementary Material. The hydrogen gas used was industrial grade (assay: 99.5%) from cylinders. All gas flow rates were controlled using Alicat mass flow controllers.

The wider flammability range of hydrogen compared with natural gas means as the hydrogen fraction is increased the fuel mixture's flammability limits widen and less air is required to form a combustible mixture inside the burner head. Additionally, the increase in volumetric fuel flow required to maintain heat input for larger fractions of hydrogen will entrain more primary air, pushing the equivalence ratio closer to stoichiometric [22]. Consequently, the likelihood of flashback is predicted to increase for each increase of hydrogen in the fuel stream. Initially, hydrogen fraction was increased by 10 vol% for each fuel injector diameter until flashback (or other undesirable characteristic) — once the safe limits for hydrogen addition were established, a select set of hydrogen-natural gas fuel blends were more closely examined for their impact on the key performance criteria of the burner. The combinations of fuel injector size and primary air entrainment settings considered are outlined in Table 1.

Hydrogen was added to the AN-burner without any modification to injector diameter is considered while allowing either maximum air entrainment (A4 cases), that is, with the air chamber open, or no air entrainment via closing the air chamber (non-premixed, NP cases). The NP cases refer to a simple non-premixed flame where no primary air can be entrained. For many applications, primary air contributes to other factors beyond just the stoichiometry of the fuel mixture, such as critical cooling of the burner. In these applications, complete restriction of primary air may not be possible and hence, modification strategies which do not completely restrict primary air are incorporated into the scope of this investigation. Two additional jet diameters are considered, an 8 mm (A8) and 12 mm (A12) jet diameter, both allowing full air entrainment.

Diagnostics

A variety of diagnostic equipment was used to measure the impact of hydrogen and burner modifications on relevant performance parameters.

Chemiluminescence data of the OH* radical was collected for full flame profiles. OH* only occurs within the reaction

Table 1 – Burner operating conditions and respective case codes.

Code	H_2 (vol%)	Air entrainment	d_{jet} (mm)
H000-A4	0	Full	4
H010-A4	10	Full	4
H050-A4	50	Full	4
H000-NP	0	Non-premixed	4
H010-NP	10	Non-premixed	4
H050-NP	50	Non-premixed	4
H090-NP	90	Non-premixed	4
H100-NP	100	Non-premixed	4
H010-A8	10	Full	8
H050-A8	50	Full	8
H090-A8	90	Full	8
H010-A12	10	Full	12
H050-A12	50	Full	12
H090-A12	90	Full	12
H100-A12	100	Full	12

Please cite this article as: Gee AJ et al., Hydrogen addition to a commercial self-aspirating burner and assessment of a practical burner modification strategy to improve performance, International Journal of Hydrogen Energy, https://doi.org/10.1016/j.ijhydene.2023.06.230

zone, which makes for an ideal marker of parameters such as reaction zone location and flame length. The isolation of OH* to the reaction zone allows for analysis separate from the ambiguity associated with other techniques. OH* chemiluminescence was captured with an ICCD camera using a 50 mm f/3.5 UV lens through a 310 nm bandpass filter (FWHM = 10 nm). The OH* images are presented in green false colouration, to distinguish them from true-colour images. A DSLR camera (Canon EOS 6D) with a 50 mm lens was used to capture flame photographs. All photos were taken with a 3.2 s exposure time, an aperture of f/22 and white balance of 4900 K. An ISO sensitivity of either 100, 400 or 800 was chosen to accommodate for the differing brightness of the flames, image meta data is documented for all flame photographs in the respective figure captions. The hydrogen flames appeared orange, attributed to sodium impurities from the air, as has been reported previously [42,43]. To eliminate this uncontrolled artefact, imaging was through a 594-nm (23-nm full-width at half maximum) notch (NTC) filter to eliminate the orange colour. Spectrometry data, included in Fig. S1 of the Supplementary Material, shows a peak at 589 nm, corresponding to the well-known sodium emission lines, and photographs with and without the notch filter are shown for comparison. Fig. S1 in the Supplementary Material also shows the OH* chemiluminescence at 310 nm.

Photograph scale bars are provided on true-colour and OH* chemiluminescence figures to provide a sense of scale for flame length. Additionally, OH* chemiluminescence flame lengths are provided in a separate figure (Fig. 7) which are defined at the axial distance along the flame centreline at which signal intensity from OH* chemiluminescence falls below 50% of the measured peak intensity. The time-averaged OH* images presented in this work are statistically stationary, however, due to the turbulent nature of the flames, the variability in the spatial location of the flame brush leads to a smearing of the mean OH* signal. The 50% intensity threshold was found to ensure consistency with the determination of the flame length whilst reducing the effects of noise. The exact value of the threshold does not affect the trends or the discussion of the results.

Axial heat flux measurements were taken using a Medtherm sensor and view restrictor positioned on a vertical traverse. The modified view angle of the sensor was 20° so that the downstream evolution of the heat flux profile could be resolved. The error is calculated as the sum of the measurement accuracy (0.5% of the reading) and the standard deviation of the sample population. Each sample is corrected by subtracting a dark charge of the laboratory on the day of collection. Radiant heat fraction is calculated using a point-radiation assumption and Eq. (2), similar to previous work [36,49,50] where the radiant fraction (χ_r) is calculated as the sum of axial heat flux measurements (Q_p) multiplied by the radiative area ($4\pi R^2$) and divided by the total heat input (Q_t) from the fuel stream. Here R is the distance from the flame centreline to the sensor.

$$\chi_r = \frac{Q_r}{Q_t} = \frac{4\pi R^2 \sum Q_p}{LHV \cdot \dot{m}} \quad (2)$$

Teledyne T200/T300 gas analysers were used to measure NOx concentrations in the flue gas on a wet basis. Samples were taken from 1800 mm above the burner exit plane, inside a capture-hood to minimise dilution. The error is calculated as the sum of the measurement accuracy (0.05% of the reading) and the standard deviation of the sample population. Each sample is corrected for background readings present in the laboratory on the day of collection. Raw NOx data is corrected to 0% O_2 and converted to an emission index (EI) with units mg/MJ using Eq. (3) where n is the moles of some pollutant (e.g. NO_2) per mole of fuel and HHV is the higher heating value of the fuel blend. A more detailed derivation of Eq. (3) is provided in the supplementary material.

$$EI = \frac{n}{HHV} \quad (3)$$

Results and discussion

Impact of H_2 on burner function and effect of increased d_{jet}

Fuel momentum and equivalence ratio

The ability to predict and control the fuel/air ratio of a burner is critical to ensuring optimal combustion efficiency, stability and safety. Self-aspirating burners are designed to be operated on a specific fuel or fuel blend, such as LPG or natural gas. Fuel injector jets and air intake orifices are sized to entrain the appropriate amount of air to optimise a variety of factors including stoichiometry, velocity, and stability. Operating a self-aspirating burner on a fuel which it was not designed for can have a significant impact on performance and safety. In this case, hydrogen was added to natural gas while conserving the total heat input until the burner flashed back. Using the air chamber mentioned in Section 2.1, air supply was adjusted such that the pressure inside the chamber was equal to 0 Pa(g) for each hydrogen/natural gas fuel blend and for each fuel injector diameter, A4, A8 and A12, respectively. The

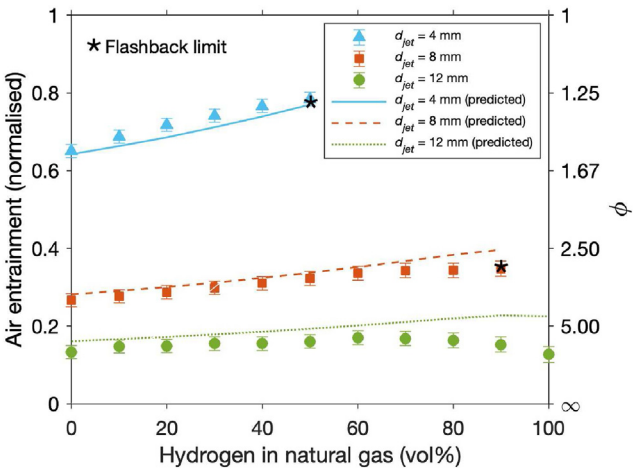

Fig. 2 – Measured (markers) and predicted (lines) volumetric air entrainment normalised to the respective stoichiometric air requirements for varying hydrogen/natural gas fuel blends at constant heat input (35 kW). The upper fraction of hydrogen addition before flashback is highlighted with asterisks (*).

Please cite this article as: Gee AJ et al., Hydrogen addition to a commercial self-aspirating burner and assessment of a practical burner modification strategy to improve performance, International Journal of Hydrogen Energy, https://doi.org/10.1016/j.ijhydene.2023.06.230

corresponding entrained air for each of the hydrogen/natural gas blends up to the point of flashback are presented in Fig. 2 as both fraction of stoichiometric air and equivalence ratio to highlight changes in stoichiometry. Predicted air entrainment values from a simple model (Eq. (1)) [18,22], described in Section 2.1 are also presented in Fig. 2.

The measured primary air entrainment for the base natural gas case was 390 SLPM, creating a rich fuel/air mixture inside the burner head with a $\varphi = 1.54$. As the hydrogen content in the fuel was increased, the total volumetric fuel flow was increased to conserve total heat input due to the lower volumetric energy density of hydrogen. This resulted in an increase in the fuel jet velocity while the fuel density decreased — consequently, there is an opposing dual action of hydrogen with respect to fuel momentum. The results in Fig. 4 show peak momentum is achieved at 80 vol% hydrogen. This is due to competing effects caused by a linear decrease in density and an exponential increase in velocity of the fuel stream as hydrogen fraction is increased. The normalised entrained air increased by 20% with the addition of 50 vol% hydrogen in the 4-mm case, entraining up to 78% of stoichiometric air, creating a fuel-air mixture inside the burner head with $\varphi = 1.27$. Overall, hydrogen addition at constant heat input had an increasing effect on primary air entrainment for each d_{jet} considered. As noted in the introduction, the addition of hydrogen also extends flammability limits and increases laminar flame speed, which both contribute to an increased propensity for flashback. The determined upper limits of hydrogen addition before flashback are discussed in Section 3.1.2 but it is noteworthy that the increased entrainment caused by the addition of hydrogen adds to the risk of flashback by pushing the fuel-air mixture closer to stoichiometric.

The impact of increasing d_{jet} has a strong reducing effect on primary air entrainment. A doubling of the d_{jet} value results in a four-fold increase in jet area and a sixteen-fold decrease in fuel momentum flux and a four-fold decrease in momentum flow. The fuel momentum in a self-aspirating design is directly proportional to the entrainment capacity of the burner [22]. The results from Fig. 4 show increasing d_{jet} to 8 mm and 12 mm changes the fuel momentum by almost an order of magnitude, which is a significantly larger impact than the change in velocity or density caused by the addition of hydrogen. The significant reduction in fuel momentum causes the fuel-air mixture inside the burner head to become significantly richer. The equivalence ratio ranges from $\varphi = 1.27–1.54$ with the 4 mm jet but increases to $\varphi = 2.88–3.75$ and $\varphi = 5.76–7.87$ for the 8 mm and 12 mm cases, respectively. The trends for experimentally measured air entrainment presented in Fig. 2 support the notion that momentum is the dominant parameter affecting entrainment in self-aspirating burners.

The results presented in Fig. 3 show a positive linear trend between entrained air and fuels-stream momentum. The trends for measured entrained air, predicted entrained air and calculated fuel stream momentum each exhibit a positive linear relationship with increasing hydrogen fraction up to ~80 vol% at constant heat input, above this the trends become non-linear up to 100 vol%. The volume of entrained air in a self-aspirating burner is often reported to be directly proportional to the momentum of the fuel stream [22] and so fuel momentum is a good predictor of the entrainment potential of a burner. To quantify how well the measured air entrainment data correlates with the calculated fuel momentum a correlation factor can be used. The Pearson Correlation Coefficient (PCC) for the measured normalised air entrainment in Fig. 2 and the calculated momentum flow in Fig. 4 is 0.985, 0.995 and 0.588 for the 4-mm-, 8-mm- and 12-mm-diameters, respectively. It is noteworthy that the correlation between the 12-mm-diameter entrained air and momentum is slightly less compared with the 4-mm and 8-mm — however, the 12-mm cases cover a greater range of hydrogen blends which do not maintain a linear trend above ~80 vol%. In fact, if the correlation coefficient for the 12-mm case is calculated excluding the 100 vol% hydrogen case, the PCC become 0.797. Further restricting the range of hydrogen

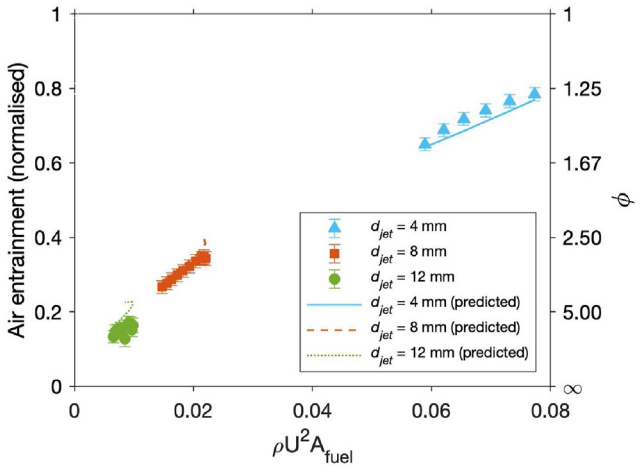

Fig. 3 — Measured (markers) and predicted (lines) volumetric air entrainment normalised to the respective stoichiometric air requirements for varying fuel-stream momentum flow values.

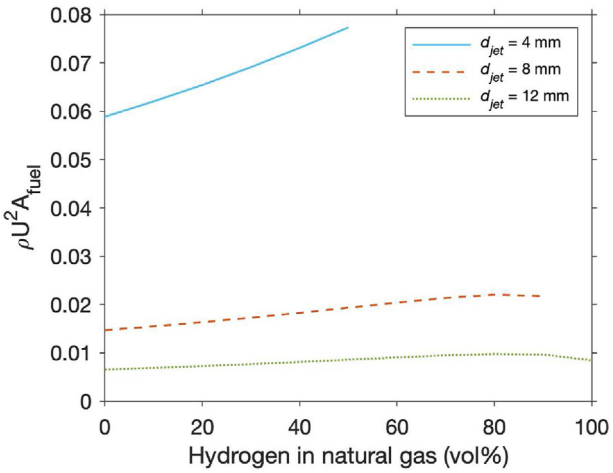

Fig. 4 — Calculated momentum flow values (at the injection point) for varying hydrogen/natural gas fuel blends at constant heat input (35 kW).

Please cite this article as: Gee AJ et al., Hydrogen addition to a commercial self-aspirating burner and assessment of a practical burner modification strategy to improve performance, International Journal of Hydrogen Energy, https://doi.org/10.1016/j.ijhydene.2023.06.230

blends (<80 vol%) continues to improve correlation with calculated momentum flow. The correlation coefficients for the predictive model with experimental results are of 0.988, 0.997 and 0.591, where, similar to momentum flow, improved correlation can be achieved by excluding experimental data for hydrogen blends >80 vol%. In general, there is a good ability for relatively simple analysis of fuel properties and burner geometry to produce the air entrainment for alternative fuels blend, but their accuracy is reduced for large fractions of hydrogen.

The lesser correlation for larger fractions of hydrogen can also be correlated with a lower Reynolds number. The influence of turbulence has been previously discussed as a factor affecting the entrainment of air in a self-aspirating burner [20,51]. The non-linear reduction in Reynolds number highlighted in Fig. S2 in the Supplementary Material may inhibit the model in Eq. (1) to predict the entrained air across a wide range of turbulent intensities. Alternatively, or additionally, the discrepancy in Fig. 2 may be related to a higher sensitivity to the aerodynamic effects of the burner geometry. The use of fuel momentum or the model in Eq. (1) only includes the density of the fuel/air streams and a simplistic assumption of co-axial geometry. Aerodynamic effects are a complex interaction of forces relating to parameters such as drag coefficient, dynamic pressure and aerodynamic design — many of which vary exponentially or otherwise non-linearly with flow properties like velocity and density. As the hydrogen fraction in the fuel is increased and the total volumetric fuel flow is increased in order to maintain the heat input, the impact of burner features like venturi-style inlets, injector recesses and non-uniform aerodynamics may become more significant leading to reduced prediction accuracy.

Flashback limits

A primary concern for hydrogen addition in partially-premixed combustion is the risk of flashback. There are several factors which are reported to increase the propensity of flashback events — hydrogen addition to natural gas lowers the stoichiometric air requirement, widens the flammability limits and increases the laminar flame speed [52]. These factors, combined with the increase in primary aeration shown in Fig. 2, all contribute to the likelihood of flashback by creating a scenario where the fuel/air mixture inside the burner head can be ignited and burn at the fuel injector instead of at the intended burner head [53].

In the present investigation, the practical limit for hydrogen addition at constant heat input was determined to be 50 vol%. Above 50 vol% the flame became increasing visually and audibly unstable, with flashback occurring after a sustained period of operating at ~60 vol% hydrogen. Flashback could be easily identified by visual inspection, where a lit-back flame is attached to the fuel injector and burning inside the burner head. Flashback also resulted in a significant increase in combustion noise as the limit is approached before a loud pop, signalling the flashback event itself, which is consistent with previously reported flashback observations [40]. Increasing d_{jet} to 8 mm extended the safe operating limit of hydrogen to 90 vol%, the 8-mm-jet flashed back after a short period of sustained operation near 100 vol% hydrogen. Further increasing d_{jet} to 12 mm allowed for stable operating of up to 100 vol% hydrogen without flashback at all.

It should be noted that burner surface temperature has been shown to be a contributing factor to flashback propensity in some burners [16,54]. The high cross-sectional to surface area ratio of the burner head allows for sufficient cooling of the burner surface to not contribute to flashback. Furthermore, each flame was allowed to operate for a sustained period of time to ensure operational equilibrium was achieved. Although an analysis of burner surface temperature was beyond the scope of this investigation, it will be included as a topic in upcoming future work on the flashback propensity in hydrogen-blended flames.

The simple modification of fuel injector size may be a practical solution to overcome the issue of flashback. In this investigation, primary air was reduced by increasing d_{jet} from 4 mm to 8 mm and 12 mm. The larger jet diameters extend the blending limits of hydrogen before flashback from 50 vol% to 90 vol% and 100 vol%, for 8 mm (A8) and 12 mm (A12) cases, respectively. These flashback limits are used as the fuel blends to be investigated in more detail. The following sections consider a base case (NG), two milestone blending points (10 and 100 vol% H_2) and critical limits of hydrogen addition before flashback (50 vol%, 90 vol% H_2).

It should be noted that although this investigation is primarily concerned with the steady state flashback limit, due to the large reduction in fuel jet velocity, the impact on the turndown limit is also quantified for the H000-A4 and H100-A12 cases and presented in Table 2. Turndown refers to operation of the burner with a sub-maximal heat output. Many commercial burner designs feature user-controlled gas supply, often in the form of control dials or "low" settings. Although not the focus of this investigation, it is an important limitation to recognise for the practical implementation of strategies which lower jet velocity. That is, the operation of the modified burner with hydrogen has a much smaller turndown ratio than the unmodified burner on natural gas.

Performance of H_2-blended flames in the modified burner

Flame appearance

Flame length and visibility are important characteristics that may be impacted by hydrogen blending. To quantify these effects, true-colour photographs and OH* chemiluminescence images have been collected, as described in Section 2.3. As hydrogen content in the fuel is increased, the flammability limits of the fuel mixture are widened. Furthermore, the primary air entrainment is increased. In combination, the propensity for flashback is increased. Initially, hydrogen fraction was increased by 10 vol% for each fuel injector diameter until

Table 2 – Turndown limits before flashback as minimum heat input values and percentage of maximum heat input.

Code	Heat input (kW)	Fraction of maximum heat input (%)
H000-A4	4.2	11.9
H100-A12	18.8	53.7

Please cite this article as: Gee AJ et al., Hydrogen addition to a commercial self-aspirating burner and assessment of a practical burner modification strategy to improve performance, International Journal of Hydrogen Energy, https://doi.org/10.1016/j.ijhydene.2023.06.230

flashback (or other undesirable characteristic) — once the safe limits for hydrogen addition are established, a select set of hydrogen-natural gas fuel blends are more closely examined for their impact on the key performance criteria of the burner. The combinations of fuel injector size and primary air entrainment settings considered are outlined in Table 1 (a pure natural gas, a pure hydrogen case, and 10 vol%, 50 vol% and 90 vol% blended cases). At each blending ratio, the flame is presented as a split image, corresponding to with and without air entrainment, on the left- and right-hand side of each of the images in the figures. In the 90 vol% and 100% hydrogen cases where an aerated flame was not stabilised due to flashback, only the cases without air entrainment are presented. Fig. 5a shows true-colour images and Fig. 5b shows OH* chemiluminescence images for hydrogen addition to natural gas with the base (4-mm-diameter) fuel injector.

Presentation of both true-colour and OH* chemiluminescence flame image data allows for a multifaceted look at the effects of hydrogen addition and d_{jet} modification. Flame images presented in Fig. 5a indicate that hydrogen addition reduces the visible flame length. Hydrogen addition reduces visibility of true-colour flame images and increases the intensity of OH* chemiluminescence images. A substantial increase in flame length can be seen in Fig. 5a and b for the non-premixed (NP) cases compared with the base (A4) cases. The relative reductions in visible flame length for non-premixed (NP) cases have been shown previously for smaller laminar flames [45]. The typical blue and yellow colouration of natural gas flames changed with increased hydrogen content, tending to a purple colour with 90 vol% hydrogen and a pale red colour at 100 vol% hydrogen. Closing the primary air supply resulted in an increase in yellow/orange colour of the flames with up to 50 vol% hydrogen, as expected due to the increase in soot formation corresponding to the non-premixed flame configuration [45,55]. The increase in soot volume fraction in richer fuel/air mixture flames is expected to result in increased radiation heat transfer, which will be investigated and quantified in Section 3.2.2. For the cases with no aeration (NP), the 0%, 10% and 50% flames initially appeared to be lifted from the burner however, no lift-off is observed for any flames in OH* chemiluminescence images (Fig. 5). Overall, hydrogen addition and increasing d_{jet} have a strong influence on the flame length and visibility. Further analysis and discussion of flame length is reported later in this section (Section 3.2.1).

The base case (H000-A4) natural gas flame was entirely blue in colour, changing to yellow/orange when the primary air was restricted (the H000-NP case). Near flashback, at 50 vol % hydrogen, the flame took on two distinct regions, a bright blue inner core and pale blueish-red outer plume. This can also be seen in the OH* chemiluminescence data in Fig. 5b. A strong chemiluminescence signal is observed in the core of the 50 vol% (A4) flame, surrounded by a lower-intensity outer plume. This observation is unique to the H050-A4 flame case, not seen in any of the other flames. The existence of a two-zoned flame has been known for many years and has been previously described as the result of unreacted fuel mixing

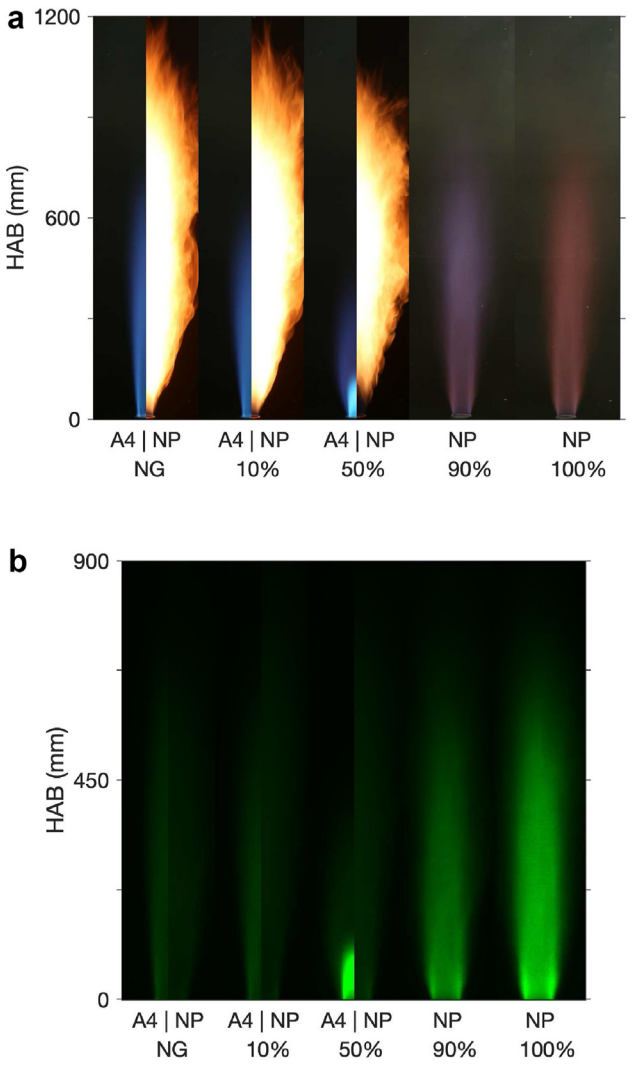

Fig. 5 — a: Photographs of flames at different volume percentages of hydrogen blended with natural gas (NG) (up to 100% H_2). Constant heat input (35 kW) through a 4 mm fuel injector. Air entrainment is indicated as either full (A) or none (NP). Where blending ratios produced a stable flame for both types of air entrainment, the A and NP cases are presented as a split image. Height above burner (HAB) indicates physical scale. Exposure time: 3.2 s. White balance: 4900K. Photographs have ISO settings of 400/100, 400/100, 400/100, 800, 800, respectively. b: OH* chemiluminescence images of flames at different volume percentages of hydrogen blended with natural gas (NG) (up to 100% H_2) through a 4 mm fuel injector. Air entrainment is indicated as either full (A) or none (NP). Where blending ratios produced a stable flame for both types of air entrainment, the A and NP cases are presented as a split image. Height above burner (HAB) indicates physical scale. Photographs taken using 50 mm lens and 310 nm bandpass filter. Exposure time: 3 s. A height above burner (HAB) scale also is provided.

Please cite this article as: Gee AJ et al., Hydrogen addition to a commercial self-aspirating burner and assessment of a practical burner modification strategy to improve performance, International Journal of Hydrogen Energy, https://doi.org/10.1016/j.ijhydene.2023.06.230

with secondary air to form a second outer reaction zone [20]. Consider a rich but combustible fuel and air mixture, such as the fuel and entrained primary air in a self-aspirating burner. Initially, the mixture will react and consume all of the primary air but the unreacted or partially reacted fuel (e.g. carbon monoxide) will escape the reaction zone since the initial fuel/air mixture was too rich to ensure complete consumption of the fuel. As this unreacted mixture escapes the initial/central reaction zone, it can react with secondary atmospheric air, producing a secondary, outer reaction zone [20]. Additional factors such as the wider flammability limits and preferential diffusivity of hydrogen may contribute to this effect to produce the distinct two-zoned flame observed for the H050-A4 flame case in Fig. 5a.The notion of a double reaction zone was also been reported previously by Naha et al. [39] who described how partially-premixed flames can be classified into two distinct flame regimes, namely, a double flame and a merged flame. In this case, it was reported that a double flame region is induced by a relatively low equivalence ratio and low strain rate, with the flame transitioning to a merged flame as primary air and/or strain rate is increased [39]. This is also consistent with the present observations, where for the 50 vol % hydrogen case, where the double flame region is observed, the equivalence ratio is reduced by 17% and fuel jet velocity, which is related to strain rate, is increased by 53% relative to natural gas. Physically separate reaction zones imply a non-uniform temperature profile which may have a significant effect on NOx emissions.

Since increasing d_{jet} is an effective means of extending the blending limits of hydrogen in natural gas, its effect on flame length and visibility also requires investigation. The impact of increasing d_{jet} is presented as photographs and OH* images for the 8- and 12-mm jet cases, in Fig. 6a and b, respectively. Each image is split between the 8-mm-diameter and 12-mm-diameter fuel injectors, on the left- and right-hand side of the images, respectively.

The partial reduction in primary air caused by increasing d_{jet} (Section 3.1.1) produced flames which appeared as intermediates between the A4 and NP cases. Overall, flame visibility increased as primary air was reduced, due to an increase in soot formation from A4 to A8, A12 and NP, consistent with the reduction in primary aeration. The colour of the 90 and 100 vol% hydrogen flames was not affected between NP, A8 and A12 cases — although, the colour intensity increased with the addition of primary air. It is noteworthy that the inception of the yellow/orange colour, which is assumed here to indicate soot, was first observed at the end of the flame.

Both visible and OH* chemiluminescence flame length appear to be highly sensitive to both hydrogen fraction and primary aeration. Flame length is a critical metric to consider when making changes to a burner design or the properties of fuel. Knowledge of how flame length is impacted by the intricate relationships between fuel composition and air stoichiometry is critical to practical applications. In applications where a flame is a part of a larger system such as a commercial oven or kiln, a change in flame length may result in the combustion reaction taking place in zones where it is not desired or heat protection is not present or where operators are working. Inferring how the flame length can be affected if fuel composition or primary aeration is changed is a useful tool for practical implementation of the methods investigated in this work and knowledge of how flame length will be affected and strategies to replicate the properties of existing NG flames is critical to minimising the impact of a transition toward hydrogen.

In addition to the visible flame length scale provided on Figs. 5a and 6a, OH* chemiluminescence flame images are used (in Figs. 5b and 6b) to provide an alternative perspective. Chemiluminescence of the OH* radical is particularly well suited to measuring flame length at it only occurs within the reaction zone, and thus avoids ambiguity associated with other techniques. To highlight the effect of hydrogen addition on the burner modifications considered, a plot of OH* chemiluminescence flame length is presented in Fig. 7. Additionally, to highlight the effect of changing the aeration, a plot of OH* flame length normalised to the base case (H000-A4) is presented in Fig. 8 as a function of fraction of stoichiometric air supplied.

The natural gas base case (H000-A4) has an OH* chemiluminescence flame length of 620 mm which is in good agreement with true-colour images presented in Fig. 5a. As hydrogen was added under the full air operating conditions (A4), the OH* flame length decreased by 9% and 18% for H010-A4 and H050-A4 flames, respectively. Similar decreases in flame length have been reported previously with hydrogen addition, in addition to the aforementioned change in colour to a pale red flame [40].

The OH* flame lengths presented in Figs. 7 and 8 highlight some discrepancies, where some OH* flame lengths are notably shorter than their true-colour alternatives presented in Figs. 5a and 6a. In particular, highly sooting flames such as the NP cases (0–50 vol% hydrogen) which were much more visible as a result of the increase soot content. The presumed increase in soot volume fraction is most likely the cause of these discrepancies. The higher soot content of these flames is not well-represented by the OH* chemiluminescence data since soot typically forms in locations of fuel-rich combustion, whereas OH* typically forms in fuel-lean regions of the flame. Consequently, increases in flame length as a result of increased soot content are not shown in the OH* flame length analysis.

Fig. 8 shows that the degree of premixing had a strong, non-monotonic influence on OH* flame length. For 10, 50 and 90 vol% blends, OH* flame length initially increased as primary air was added, peaking after addition of ~15% of stoichiometric air at 1.2–1.4 times the length of the base (H000-A4) natural gas case. As the mixture became leaner, >15% of stoichiometric air, flame length decreased, with the shortest flame lengths resulting from the leanest fuel blends. This is primarily a result of a lower requirement to entrain secondary atmospheric air to achieve a local stoichiometric mixture, which reduces residence time for complete combustion [56,57]. As the fuel/air mixture inside the burner head approaches stoichiometric conditions ($\varphi = 1$), the combustion reaction can occur at a reduced residence time and consequently, reduced flame length. Additional/alternative contributing factors to the reduced flame length of hydrogen-blended flames may be an increased molecular diffusivity of hydrogen compared to natural gas which has been previously reported to contribute to a reduced flame length [45,58–60].

Please cite this article as: Gee AJ et al., Hydrogen addition to a commercial self-aspirating burner and assessment of a practical burner modification strategy to improve performance, International Journal of Hydrogen Energy, https://doi.org/10.1016/j.ijhydene.2023.06.230

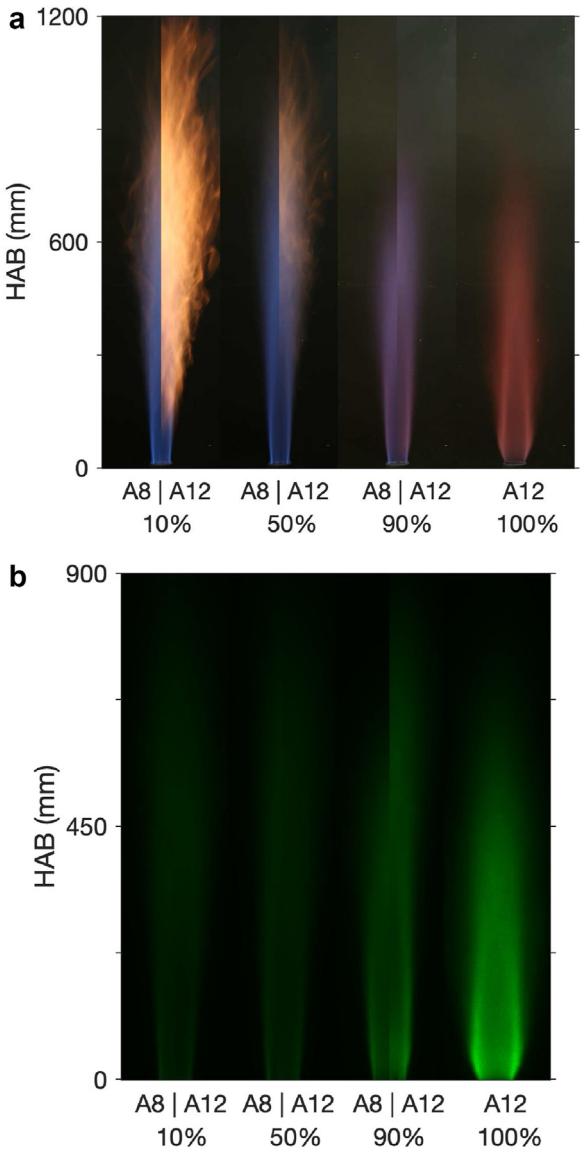

Fig. 6 – a: Photographs of flames at different volume percentages of hydrogen blended with natural gas (NG) (up to 100% H_2). Constant heat input (35 kW) through an 8 mm (A8) or 12 mm (A12) fuel injector. Full air entrainment (A) is permitted for each flame. Where blending ratios produced a stable flame for d_{jet} values, the A8 and A12 cases are presented as a split image. Height above burner (HAB) indicates physical scale. Exposure time: 3.2 s. White balance: 4900K. Photographs have ISO settings 400/400, 400/400, 800/800, 800, respectively. b: OH* chemiluminescence images of hydrogen addition to natural gas (NG) by different volume percentages at constant heat input (35 kW) through an 8 mm (A8) or 12 mm (A12) fuel injector. Full air entrainment (A) is permitted for each flame. Where blending ratios produced a stable flame for djet values, the A8 and A12 cases are presented as a split image. Height above burner (HAB) indicates physical scale. Photographs taken using 50 mm lens and 310 nm bandpass filter. Exposure time: 3 s. A height above burner (HAB) scale also is provided.

Overall, the impact of hydrogen on flame visibility was significant for blends with 90 vol% hydrogen or more, where the flame became less visible and changed to a purple/red colour. Increasing d_{jet} did improve flame visibility, presumably due to a slower oxidation of methane and resulting increased soot formation and luminosity, for blends with lower hydrogen content. However, for the 90 vol% hydrogen blend visibility was low since there was very little carbon in the fuel and for 100% hydrogen which has no capacity to generate soot.

The measured flame lengths follow non-monotonic trends with percent of hydrogen in the fuel and d_{jet} values considered in this investigation. Primary air addition appears to have a more significant influence on reducing flame length than hydrogen addition, although both contribute to shorter flames.

Radiant heat transfer

The reduced soot formation and resulting radiant heat transfer of hydrogen-blended flames as a result of carbon displacement is a noteworthy concern for the practical implementation of hydrogen for industries which rely on radiation as a primary mode of heat transfer. Insight into the magnitude by which various hydrogen blends impact radiant heat transfer in practical combustion systems is critical to facilitating a transition away from hydrocarbon-based fuels. Similarly, the efficacy of approaches to help integrate hydrogen into existing gas infrastructure should be weighed against their impact on key performance criteria such as radiant heat transfer. This is especially relevant for strategies which affect equivalence ratio, as this is also closely linked to the radiant heat transfer capacity of premixed flames [61].

Derivatives of the AN-burner design are also used for mining and minerals processing applications, where radiant heat transfer is also an important mode of heat transfer. Radiant heat transfer is quantified by taking time-averaged heat flux samples in 200 mm vertical steps axially along each flame. The axial heat flux data are presented in Fig. 9. Additionally, to provide a more global perspective to the axial data, the overall radiant heat fractions of each flame are calculated using Eq. (2) and presented in Fig. 10.

The axial heat flux data presented in Fig. 9 displays a non-monotonic shape across all cases, peaking 300 mm downstream of the burner exit plane. The radiant heating fraction of all flames is between 10 and 20% of total heat input. The axial heat flux of the base case (H000-A4) peaked at 0.34 kW/m^2. The percentage of total heat output coming from radiation in the H000-A4 case was 13%. The addition of hydrogen under the base case (A4) operating conditions had a negligible effect up to 10 vol% on the axial heat flux profile and overall radiant heating fraction, which reduced to less than 12%. A negligible effect on radiant heat transfer with the addition of 10 vol% hydrogen is consistent with the majority of previous work [45]. The addition of 50 vol% hydrogen using the 4-mm injector caused a notable change in axial heat flux profile, although this resulted in a negligible overall impact on radiant heating fraction. The H050-A4 flame had a significantly shorter axial profile and exhibited a high peak heat flux in the initial 200-mm of the flame. The OH* chemiluminescence data for the H050-A4 case also showed a significantly shorter flame length

Please cite this article as: Gee AJ et al., Hydrogen addition to a commercial self-aspirating burner and assessment of a practical burner modification strategy to improve performance, International Journal of Hydrogen Energy, https://doi.org/10.1016/j.ijhydene.2023.06.230

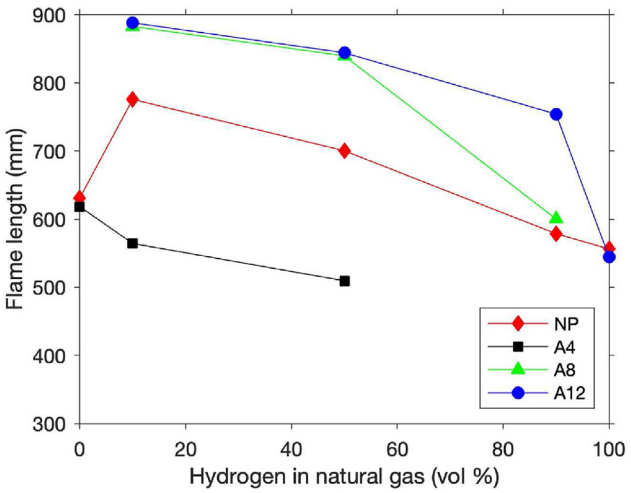

Fig. 7 – OH* chemiluminescence flame lengths for hydrogen addition to addition to natural gas (NG) by different volume percentages at constant heat input (35 kW) through a 4 mm, 8 mm or 12 mm jet, allowing either full (A) or no (NP) air entrainment. Flame length is defined here as the axial distance along the flame centreline at which signal intensity from OH* chemiluminescence falls below 50% of the measured peak intensity.

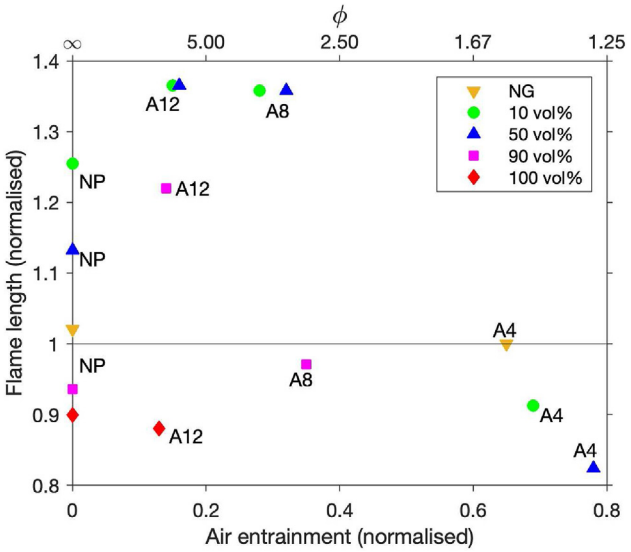

Fig. 8 – Normalised OH* chemiluminescence flame lengths for various hydrogen addition (v/v %) ratios to natural gas (NG) in a 35 kW self-aspirating burner. Flame length is normalised to the base case (H000-A4) and presented as a function of the primary air entrained (normalised to the stoichiometric requirement).

and a peak chemiluminescence intensity in the initial 200 mm of the flame (Fig. 5a and b).

The reduction (A8, A12 cases) or complete absence (NP cases) of primary air entrainment had a significant impact on the radiant heat transfer of flames. Importantly, these modifications enabled an increase in the blending ratio of hydrogen. The 8-mm-diameter injector enabled up to 90 vol% hydrogen before flashback — this resulted in an increase in peak heat flux with aeration relative to the base natural gas case (H000-A4) and the other fuel blends (H010-A8 and H050-A8) considered for the 8-mm-diameter. The H090-A8 flame case had a slight (2%) increase in overall radiant fraction, compared with the base (H000-A4) case. Increasing d_{jet} to 12 mm enabled operation of a pure hydrogen flame which produced a radiant fraction 10% lower than the base case (H000-A4) despite a good replication of the axial heat flux profile. It is interesting to note that the radiant fraction of the H100-A12 flame does not differ significantly from the 10 or 50 vol% A4 cases despite a noteworthy reduction in radiant fraction compared to natural gas. It is also worth noting that the elimination of primary aeration (NP) produced the highest heat flux measurements across all cases up to 90 vol% hydrogen, due to the presence of soot, whereas for 100 vol% hydrogen the aerated case, H100-A12, yielded a 7% more radiant flame. In other words, for 0–90 vol% hydrogen cases, the addition of primary air resulted in a decrease in radiant fraction, whereas, for the pure hydrogen flames, a partially-premixed flame had a higher radiant fraction then a diffusion flame. The result for the H100-NP case is unlikely to be related to changes in flame length since the visual and chemiluminescence flame lengths are similar. Instead, it is most likely that the addition of primary air to the non-premixed H100-NP case pushed the reaction closer to $\varphi = 1.1$, where adiabatic flame temperature typically peaks [62]. The only radiative species in pure hydrogen combustion is water. If complete combustion is assumed and all hydrogen in converted to water vapour, an increase in adiabatic flame temperature may increase radiant heat transfer.

Adjusting the fuel composition and burner geometry changes the combustion stoichiometry. As hydrogen fraction increases, the stoichiometric air requirement is reduced while the physical entrainment of air is increased due to the added momentum (refer Section 3.1.1). To more clearly analyse how the underlying changes in stoichiometry, caused by increases in hydrogen fraction and d_{jet}, affect the radiant heating properties of the flames, the radiant heating fraction of each flame is normalised against the base natural gas (H000-A4) case and plotted against the percentage of stoichiometric air entrained, as measured in Section 3.1 for each fuel blend and d_{jet} value. The results are presented in Fig. 11.

Fig. 11 shows that there is a general trend for each fuel blend, with some exceptions, that increasing the fraction of stoichiometric air supplied decreases the radiant fraction. Simple dilution effects may contribute to this observation, however, the reduced soot volume fraction as a result of partial premixing and greater oxidation may also contribute. Note that the rate at which addition of primary air reduces heat flux decreases as hydrogen fraction increases —in fact, at 100 vol% hydrogen, the normalised radiant fraction increased by 8% with the addition of 13% of stoichiometric air.

The trends observed in Fig. 11 highlight that increasing either hydrogen fraction or primary air entrainment caused a reduction in the radiant fraction of the flames. These results are consistent with similar investigations [63] where hydrogen-enriched flames increased their radiative heat

Please cite this article as: Gee AJ et al., Hydrogen addition to a commercial self-aspirating burner and assessment of a practical burner modification strategy to improve performance, International Journal of Hydrogen Energy, https://doi.org/10.1016/j.ijhydene.2023.06.230

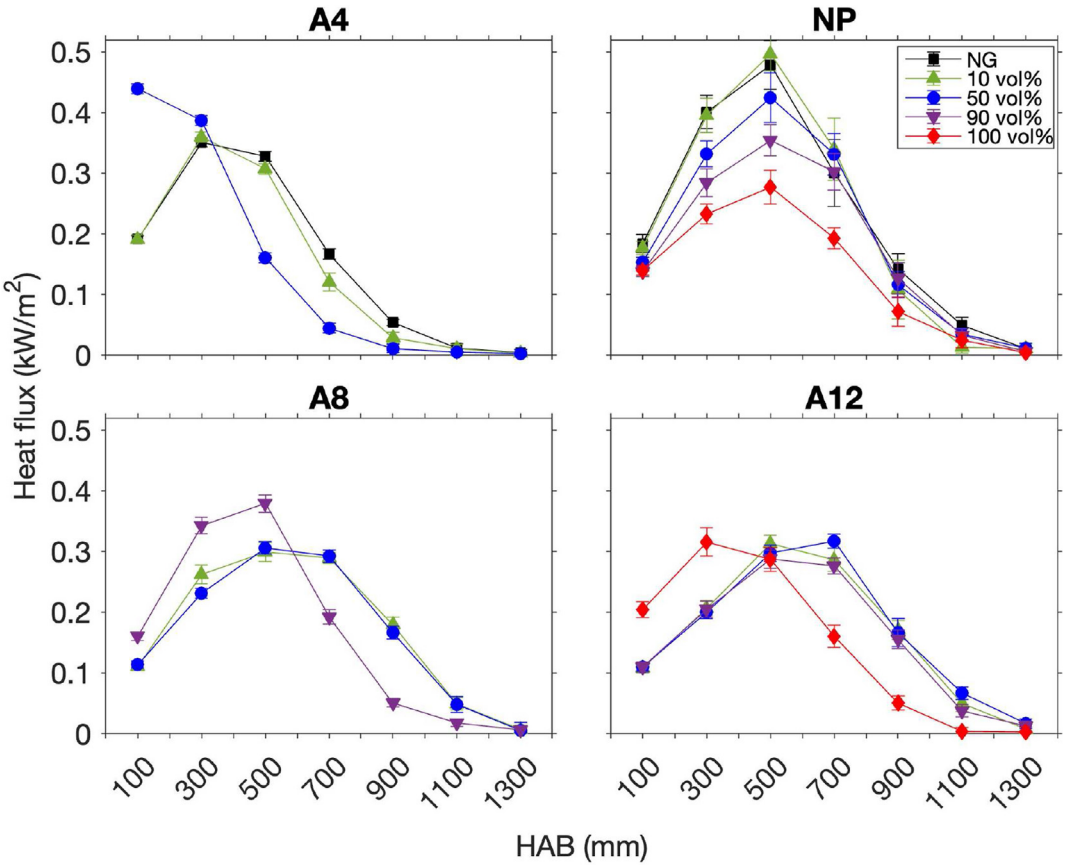

Fig. 9 – Axial heat flux measurements for hydrogen addition to natural gas (NG) in a 35 kW self-aspirating burner, where A4 represented a 4 mm fuel jet allowing full air entrainment, NP represents a 4 mm fuel jet allowing no air entrainment, A8 represents an 8 mm fuel jet allowing full air entrainment and A12 represents a 12 mm fuel jet allowing full air entrainment.

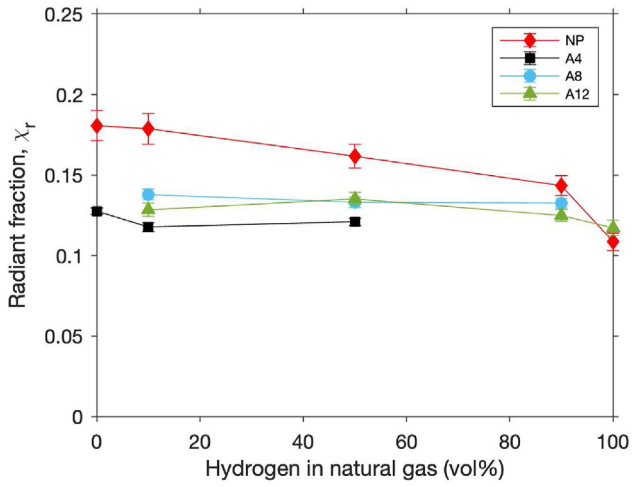

Fig. 10 – Radiant heat fraction for hydrogen addition (v/v %) to natural gas (NG) in a 35 kW self-aspirating burner with a 4 mm, 8 mm or 12 mm jet, allowing either full (A) or no (NP) air entrainment.

transfer as the fuel/air mixtures became richer (φ = 1–3). It should also be noted that this study [63] demonstrated a strong influence of the Reynolds number at the fuel jet with respect to the impact of equivalence ratio. The reducing effect of hydrogen on thermal efficiency was shown to increase for low Reynolds numbers (Re = 300–500) and low equivalence ratios (φ = 1–3) [63]. This is especially significant since, to increase the fraction of hydrogen in a fuel mixture while conserving heat input, Reynolds number and equivalence ratio decrease as a result of reduced fuel density and a combination of increased air entrainment and lower requirement for stoichiometric air, respectively. A table of Reynolds numbers calculated for each d_{jet} value is presented in Fig. S2 of the Supplementary Material.

In summary, hydrogen blending reduces radiant heat transfer, which is consistent with previous investigations [45]. Increasing d_{jet} to 8 mm, which permitted up to 90 vol% hydrogen blending without flashback, resulted in a 2% increase in radiative heat transfer, compared with the 4 mm natural gas base case (H000-A4). A further increase in d_{jet} to 12 mm, which permitted operation with 100 vol% hydrogen without flashback, resulted in a 10% reduction in radiant heat transfer compared to the base case (H000-A4). Operating the burner under a non-premixed regime (NP cases) increased radiant heat transfer compared to cases where air was permitted, except for 100 vol% hydrogen, in which radiant heat transfer increased by 8% from H100-NP to H100-A12.

Overall, increasing d_{jet} to permit operation with hydrogen without flashback did not negatively impact radiant heat

Please cite this article as: Gee AJ et al., Hydrogen addition to a commercial self-aspirating burner and assessment of a practical burner modification strategy to improve performance, International Journal of Hydrogen Energy, https://doi.org/10.1016/j.ijhydene.2023.06.230

transfer. In fact, the resulting reduction in primary air is shown to improve the radiant properties in all flames (except the 100% hydrogen case) — with an inverse-linear correlation observed. This is a result of several factors but primarily an increase in soot formation due to a rich combustion of natural gas. The increased radiant heat transfer in the pure hydrogen flame due to primary air addition is likely a result of improved combustion, higher temperatures, and increased conversion of H_2 to H_2O, which is the main radiative species present.

NOx emissions

Hydrogen-enriched combustion is well-documented to increase NOx emissions via the thermal route, primarily due to an increase in adiabatic flame temperature [35,64–67]. NOx emissions have also been shown to be highly sensitive to equivalence ratio due to its effect on flame temperature, with NOx emissions frequently reported to peak at $\varphi = 1.0–1.1$ [68,69]. Results presented in Section 3.1 showed that the addition of hydrogen to a self-aspirating burner can significantly impact the entrainment of air and the resulting stoichiometry of the mixture.

Quantifying the impact of hydrogen blending on NOx emissions for specific burner designs is a critical step toward the adoption of hydrogen in commercial heating applications. Similarly, proposed strategies for assisting the adoption of hydrogen should be examined for their collateral effects on all performance criteria, including NOx emissions. The effectiveness of increasing fuel injector size is weighed against its impact on other performance criteria such as radiant heating capacity and NOx emissions. In the present study, NOx measurements were taken 1800 mm above the burner inside a hood to minimise dilution. Data is presented as an emission index (mg/MJ), calculated using Eq. (3). The NOx emission index is presented in Fig. 12 for all flame cases. Additionally, to provide further insight into how the changes in stoichiometry induced by increasing d_{jet} affect NOx relative to the base natural gas case, normalised NOx measurements are plotted as a function of fraction of stoichiometric air in Fig. 13.

The base natural gas (H000-A4) case produced approximately 22 mg/MJ of NOx emissions. Hydrogen addition up to 50 vol% to the unmodified (A4) burner had a negligible effect on NOx compared with the base natural gas case. Previous investigations have reported negligible increases in NOx emissions for hydrogen addition in self-aspirating burners, where the cause is often attributed to an external heat sink such as heat losses to the atmosphere due to open-air combustion or heat losses to the burner materials [17,18,28,38,41,42]. It is interesting to observe unremarkable variation in NOx for the H050-A4 flame considering the large disparity highlighted in the true-colour, OH* chemiluminescence and heat flux data in previous sections. In particular, a comparably large increase in OH* chemiluminescence intensity and measured increases in heat flux would suggest higher local temperatures which could be expected to increase NOx emissions. Furthermore, the low equivalence ratio of the H050-A4 compared with other cases would also be expected to produce some level of differentiation in measured NOx. Fig. 13 highlights a negative relationship between primary aeration and NOx emissions for all fuel blends.

Increasing d_{jet} as a means of extending the operating limits of hydrogen before flashback resulted in a reduction in primary air and a measured increase in NOx emission. This increase in NOx emissions can be considered separate or in addition to the increase caused for hydrogen addition since variation in d_{jet} in Fig. 12 or equivalence ratio in Fig. 13 even when hydrogen fraction is held constant. The data presented in Fig. 12 shows that addition of hydrogen up to 50 vol% under unmodified conditions increases NOx emissions by 1% (negligible in the context of experimental error) relative to the base (H000-A4) natural gas case, whereas addition of 50 vol%

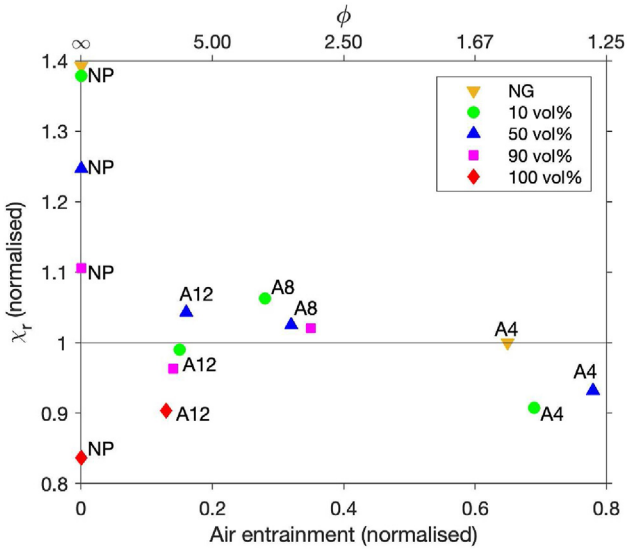

Fig. 11 – Radiant heat fraction (χ_r) for various hydrogen addition (v/v %) ratios to natural gas (NG) in a 35 kW self-aspirating burner. Radiant heat fraction is normalised to the base case (H000-A4) and presented as a function of the primary air entrained (normalised to the stoichiometric requirement).

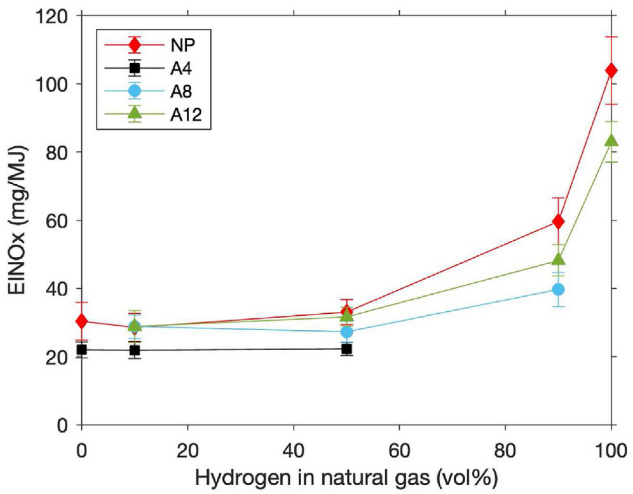

Fig. 12 – Measured NOx emission index for hydrogen addition to natural gas in a 35 kW self-aspirating burner with a 4 mm, 8 mm or 12 mm jet, allowing either full (A) or no (NP) air entrainment.

Please cite this article as: Gee AJ et al., Hydrogen addition to a commercial self-aspirating burner and assessment of a practical burner modification strategy to improve performance, International Journal of Hydrogen Energy, https://doi.org/10.1016/j.ijhydene.2023.06.230

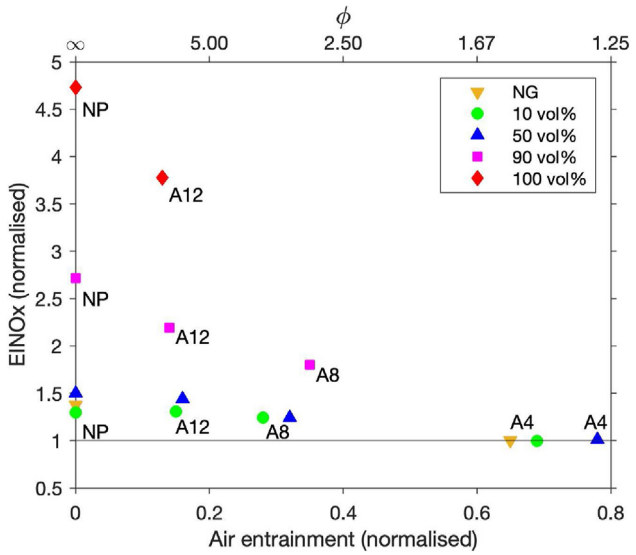

Fig. 13 – Normalised NOx emission index for various hydrogen addition (v/v %) ratios to natural gas (NG) in a 35 kW self-aspirating burner. NOx data is normalised to the base case (H000-A4) and presented as a function of the primary air entrained (normalised to the stoichiometric requirement).

hydrogen without primary air entrainment (H050-NP) results in a 50% increase relative to the H000-A4 case. Above 50 vol%, the effect of hydrogen became non-negligible. Relative to the base case, NOx emission rates increased by 80% and 280% for H090-A8 and H100-A4 cases, respectively. The NOx-increasing effects of lowering primary air also became more significant for larger hydrogen fractions, with the highest NOx emission rates being recorded for NP cases, followed by A12 and A8 cases.

The negative relationship between primary aeration and NOx emissions is surprising given a fuel/air mixture closer to $\varphi = 1.0–1.1$ is expected to increase adiabatic flame temperature and NOx formation [68,69]. Similar results have been reported previously [70], where NOx emissions increased as the mixture became richer but this testing was done at much leaner conditions ($\varphi = 0.2–0.5$) and may not be indicative of the conditions in the present investigation. The cause for the negative relationship between NOx and primary air may also be related to dilution effects. A higher amount of air dilution increases the amount of excess air—which does not participate in the combustion reactions—therefore acting as a diluent. In contrast, when air dilution is reduced the higher flame temperature may increase thermal NOx production. This notion is supported by the observation that the heat release, discussed in Section 3.2.2, also decreases for a given fuel blend as primary air entrainment is increased. The increased supply of cold fuel and air may also contribute to a cooling of the burner components, which has been previously correlated with reductions in NOx emissions [71,72] — however, these effects are unlikely to be significant in the present investigation since the burner head maintained a relatively cool state during operation.

Other or additional contributing factors may be the increased flame length in reduced-air flames highlighted in Section 3.2.1 — an increase flame length will increase residence time which has been previously reported as an important parameter in the formation of NOx [73]. Reduced NOx emissions as a result of decreased flame length have been documented previously where the underlying cause was reported as a combination of reduced residence time and a reduction in volume of the reaction zone [74].

The impact of reducing primary air entrainment (via increasing d_{jet}) as a mechanism of extending the blending limits of hydrogen in natural gas resulted in an increase in NOx emissions, in addition to the increase associated with hydrogen addition alone. That is, there is a trade-off between the benefit of extending the hydrogen-blending limit and the measured increase in NOx emissions by reducing primary aeration. This highlights the potential for establishment of an optimum d_{jet} value which extends the flashback limit but does not increase NOx emissions beyond acceptable limits. The specific d_{jet} value will depending on a number of factors pertaining to application and relevant policy/regulations.

Conclusions

The addition of hydrogen to natural gas in a commercial 35 kW self-aspirating burner was investigated. Practical performance metrics were used to quantify the impact of both hydrogen blending and a low-cost, burner modification strategy, to mitigate the challenges of hydrogen. In particular, primary air entrainment behaviour, steady-state flashback limit, flame visibility and length, radiant heat transfer and flue gas NOx emissions were quantified using experimental data. The efficacy of a modified d_{jet} to extend the blending limits of hydrogen was presented with its collateral effects on these key performance criteria quantified.

1. Hydrogen addition to the unmodified burner was achievable up to 50 vol% while maintaining a stable flame. Beyond 50 vol% the flame became unstable with flashback occurring at approximately 60 vol% hydrogen. At 50 vol% hydrogen, normalised primary air entrainment increased by 20%, entraining up to 78% of stoichiometric air ($\varphi = 1.27$). This produced a significantly shorter and louder flame than the base case natural gas flame. Increasing fuel injector diameter from 4 mm to 8 mm and 12 mm extended the hydrogen-blending limit to 90 vol% and 100 vol%, respectively. The entrainment behaviour of the burner for different fuel blends and fuel injector sizes was well-predicted by the calculated momentum flow of the fuel stream and a basic model taken from literature [18,22].
2. Flame appearance was mostly unaffected by hydrogen addition up to 10 vol% in all cases. In the unmodified (4-mm injector) burner, hydrogen addition up to 50 vol% hydrogen reduced flame length by approximately half and took on a unique dual-flame appearance, however, less significant effects were observed for other cases. Increasing d_{jet} improved flame visibility due to reduced oxidation and increased luminous soot formation, which became less effective for 90 vol% hydrogen flames since

Please cite this article as: Gee AJ et al., Hydrogen addition to a commercial self-aspirating burner and assessment of a practical burner modification strategy to improve performance, International Journal of Hydrogen Energy, https://doi.org/10.1016/j.ijhydene.2023.06.230

there was very little carbon in the fuel, and irrelevant for 100% hydrogen flames. The OH* chemiluminescence flame lengths followed non-monotonic trends with hydrogen vol % and air entrainment. Primary air addition reduced flame length more significantly than hydrogen addition, although both contributed to shorter flames.

3. Radiant heat transfer from all flames was unaffected by hydrogen addition up to 10 vol%, and for most injector diameters unaffected up to 50 vol%. In general, increasing primary air entrainment caused non-linear reductions in radiant heat transfer. Manipulation of primary air entrainment was an effective strategy to increase any reductions in radiant heat transfer caused by the addition of hydrogen, with the potential for good replication of the heat transfer properties of natural gas on large fractions of hydrogen.
4. There is a noteworthy trade-off between the benefits of extending the flashback limit and increase NOx emissions. Hydrogen addition had a negligible effect of NOx emissions up to 50 vol% with significant increases observed at 90 and 100 vol% hydrogen. The reduced primary aeration resulting from increased fuel injector size correlates with an increase in NOx emissions for all cases, with the non-premixed fuel blends exhibiting the highest NOx levels overall. For applications looking to achieve high blend ratios of hydrogen while maintaining low NOx emissions, a refinement of the methods investigated in this paper is required to determine the optimal d_{jet} and resulting primary aeration.

Declaration of competing interest

The authors declare that they have no known competing financial interests or personal relationships that could have appeared to influence the work reported in this paper.

Acknowledgements

The authors would like to acknowledge the support from the Australian Research Council, The University of Adelaide and the Future Fuels CRC (RP1.4-03). The authors also thank Ben Crossman for his technical support.

Appendix A. Supplementary data

Supplementary data to this article can be found online at https://doi.org/10.1016/j.ijhydene.2023.06.230.

REFERENCES

[1] Glanville P, Fridlyand A, Sutherland B, Liszka M, Zhao Y, Bingham L, Jorgensen K. Impact of hydrogen/natural gas blends on partially premixed combustion equipment: NOx emission and operational performance. Energies 2022;15(5):1706. https://doi.org/10.3390/en15051706.
[2] Sánchez AL, Williams FA. Recent advances in understanding of flammability characteristics of hydrogen. Prog Energy Combust Sci 2014;41:1–55. https://doi.org/10.1016/j.pecs.2013.10.002.
[3] Schiro F, Stoppato A, Benato A. Modelling and analyzing the impact of hydrogen enriched natural gas on domestic gas boilers in a decarbonization perspective. Carbon Resources Conversion 2020;3:122–9. https://doi.org/10.1016/j.crcon.2020.08.001.
[4] Levinsky H. Why can't we just burn hydrogen? Challenges when changing fuels in an existing infrastructure. Prog Energy Combust Sci 2021;84:100907. https://doi.org/10.1016/j.pecs.2021.100907.
[5] Pessoa-Filho JB. Thermal radiation in combustion systems. J Braz Soc Mech Sci 1999;21(3):537–47.
[6] Hamadi MB, Vervisch P, Coppalle A. Radiation properties of soot from premixed flat flame. Combust Flame 1987;68(1):57–67. https://doi.org/10.1016/0010-2180(87)90065-4.
[7] Hutny WP, Lee GK. Improved radiative heat transfer from hydrogen flames. Int J Hydrogen Energy 1991;16(1):47–53. https://doi.org/10.1016/0360-3199(91)90059-R.
[8] Saito K, Williams FA, Gordon AS. Effects of oxygen on soot formation in methane diffusion flames. Combust Sci Technol 1986;47(3–4):117–38. https://doi.org/10.1080/00102208608923869.
[9] Sen S, Puri I. Thermal radiation modeling in flames and fires. Transport Phenonema in Fires; 2008. p. 301.
[10] Li P, Mi J, Dally B, Wang F, Wang L, Liu Z, Chen S, Zheng C. Progress and recent trend in MILD combustion. Sci China Technol Sci 2011;54(2):255–69. https://doi.org/10.1007/s11431-010-4257-0.
[11] Evans MJ, Proud DB, Medwell PR, Pitsch H, Dally BB. Highly radiating hydrogen flames: effect of toluene concentration and phase. Proc Combust Inst 2020;38(1). https://doi.org/10.1016/j.proci.2020.07.005.
[12] Gee AJ, Yin Y, Foo KK, Chinnici A, Smith N, Medwell PR. Toluene addition to turbulent H2/natural gas flames in bluff-body burners. Int J Hydrogen Energy 2022;47(65):27733–46. https://doi.org/10.1016/j.ijhydene.2022.06.154.
[13] Yin Y, Medwell PR, Gee AJ, Foo KK, Dally BB. Fundamental insights into the effect of blending hydrogen flames with sooting biofuels. Fuel 2023;331:125618. https://doi.org/10.1016/j.fuel.2022.125618.
[14] TerMaath CY, Skolnik EG, Schefer RW, Keller JO. Emissions reduction benefits from hydrogen addition to midsize gas turbine feedstocks. Int J Hydrogen Energy 2006;31(9):1147–58. https://doi.org/10.1016/j.ijhydene.2005.10.002.
[15] Choudhury S, McDonell VG, Samuelsen S. Combustion performance of low-NOx and conventional storage water heaters operated on hydrogen enriched natural gas. Int J Hydrogen Energy 2020;45(3):2405–17. https://doi.org/10.1016/j.ijhydene.2019.11.043.
[16] Aniello A, Poinsot T, Selle L, Schuller T. Hydrogen substitution of natural-gas in premixed burners and implications for blow-off and flashback limits. Int J Hydrogen Energy 2022;47(77):33067–81. https://doi.org/10.1016/j.ijhydene.2022.07.066.
[17] Zhao Y, McDonell V, Samuelsen S. Influence of hydrogen addition to pipeline natural gas on the combustion performance of a cooktop burner. Int J Hydrogen Energy 2019;44(23):12239–53. https://doi.org/10.1016/j.ijhydene.2019.03.100.
[18] Zhao Y, McDonell V, Samuelsen S. Experimental assessment of the combustion performance of an oven burner operated on pipeline natural gas mixed with hydrogen. Int J Hydrogen

Energy 2019;44(47):26049–62. https://doi.org/10.1016/j.ijhydene.2019.08.011.
[19] Zhang S, Ma H, Huang X, Peng S. Numerical simulation on methane-hydrogen explosion in gas compartment in utility tunnel. Process Saf Environ Protect 2020;140:100–10. https://doi.org/10.1016/j.psep.2020.04.025.
[20] Design of gas burners for domestic use. In: Commerce Do, editor. Letter circular No. 299. Washington DC: Bureau of Standards; 1931.
[21] Berry WM, Brumbaugh IV, Moulton GF, Shawn GB. In: Commerce Do, editor. Design of atmospheric burners. Washington DC: Bureau of Statistics; 1921.
[22] Jones HRN. The application of combustion principles to domestic gas burner design. Taylor & Francis; 1989.
[23] Namkhat A, Jugjai S. Primary air entrainment characteristics for a self-aspirating burner: model and experiments. Energy 2010;35(4):1701–8. https://doi.org/10.1016/j.energy.2009.12.020.
[24] Pritchard R, Guy J, Connor N. Handbook of industrial gas utilization: engineering principles and practice. United States: Van Nostrand Co; 1977.
[25] Syred N, Abdulsada M, Griffiths A, O'Doherty T, Bowen P. The effect of hydrogen containing fuel blends upon flashback in swirl burners. Appl Energy 2012;89(1):106–10. https://doi.org/10.1016/j.apenergy.2011.01.057.
[26] Syred N, Giles A, Lewis J, Abdulsada M, Valera Medina A, Marsh R, Bowen PJ, Griffiths AJ. Effect of inlet and outlet configurations on blow-off and flashback with premixed combustion for methane and a high hydrogen content fuel in a generic swirl burner. Appl Energy 2014;116:288–96. https://doi.org/10.1016/j.apenergy.2013.11.071.
[27] Plee SL, Mellor AM. Review of flashback reported in prevaporizing/premixing combustors. Combust Flame 1978;32:193–203. https://doi.org/10.1016/0010-2180(78)90093-7.
[28] Zhao Y, Hickey B, Srivastava S, Smirnov V, McDonell V. Decarbonized combustion performance of a radiant mesh burner operating on pipeline natural gas mixed with hydrogen. Int J Hydrogen Energy 2022;47(42):18551–65. https://doi.org/10.1016/j.ijhydene.2022.04.003.
[29] Zhao Y. Impact of increased renewable gases in natural gas on combustion performance of self-aspirating flames. In: Mechanical and aerospace engineering. Irvine: University of California; 2020.
[30] Zhao Y, McDonell V, Samuelsen S. Assessment of the combustion performance of a room furnace operating on pipeline natural gas mixed with simulated biogas or hydrogen. Int J Hydrogen Energy 2020;45(19):11368–79. https://doi.org/10.1016/j.ijhydene.2020.02.071.
[31] Sun M, Huang X, Hu Y, Lyu S. Effects on the performance of domestic gas appliances operated on natural gas mixed with hydrogen. Energy 2022;244:122557. https://doi.org/10.1016/j.energy.2021.122557.
[32] Jones DR, Al-Masry WA, Dunnill CW. Hydrogen-enriched natural gas as a domestic fuel: an analysis based on flashback and blow-off limits for domestic natural gas appliances within the UK. Sustain Energy Fuels 2018;2(4):710–23.
[33] de Vries H, Mokhov AV, Levinsky HB. The impact of natural gas/hydrogen mixtures on the performance of end-use equipment: interchangeability analysis for domestic appliances. Appl Energy 2017;208:1007–19. https://doi.org/10.1016/j.apenergy.2017.09.049.
[34] Fang Z, Zhang S, Huang X, Hu Y, Xu Q. Performance of three typical domestic gas stoves operated with methane-hydrogen mixture. Case Stud Therm Eng 2023;41:102631. https://doi.org/10.1016/j.csite.2022.102631.
[35] Cozzi F, Coghe A. Behavior of hydrogen-enriched non-premixed swirled natural gas flames. Int J Hydrogen Energy 2006;31(6):669–77. https://doi.org/10.1016/j.ijhydene.2005.05.013.
[36] Dong X, Nathan GJ, Mahmoud S, Ashman PJ, Gu D, Dally BB. Global characteristics of non-premixed jet flames of hydrogen–hydrocarbon blended fuels. Combust Flame 2015;162(4):1326–35. https://doi.org/10.1016/j.combustflame.2014.11.001.
[37] Breer B, Rajagopalan H, Godbold C, Emerson B, Acharya V, Sun W, Lieuwen T, Noble D. NOx production from hydrogen methane blends. In: Spring technical meeting of the eastern states section of the combustion. Institute; 2022. https://doi.org/10.35090/gatech/65963.
[38] Zhan X, Chen Z, Qin C. Effect of hydrogen-blended natural gas on combustion stability and emission of water heater burner. Case Stud Therm Eng 2022;37:102246. https://doi.org/10.1016/j.csite.2022.102246.
[39] Naha S, Aggarwal SK. Fuel effects on NOx emissions in partially premixed flames. Combust Flame 2004;139(1):90–105. https://doi.org/10.1016/j.combustflame.2004.07.006.
[40] Patel V, Shah R. Effect of hydrogen enrichment on combustion characteristics of methane swirling and non-swirling inverse diffusion flame. Int J Hydrogen Energy 2019;44(52):28316–29. https://doi.org/10.1016/j.ijhydene.2019.09.076.
[41] Zhen HS, Cheung CS, Leung CW, Choy YS. Effects of hydrogen concentration on the emission and heat transfer of a premixed LPG-hydrogen flame. Int J Hydrogen Energy 2012;37(7):6097–105. https://doi.org/10.1016/j.ijhydene.2011.12.130.
[42] Yangaz MU, Özdemir MR, Şener R. Combustion performance of hydrogen-enriched fuels in a premixed burner. Environ Technol 2020;41(1):2–13. https://doi.org/10.1080/09593330.2019.1656676.
[43] Kalbhor A, van Oijen J. Effects of hydrogen enrichment and water vapour dilution on soot formation in laminar ethylene counterflow flames. Int J Hydrogen Energy 2020;45(43):23653–73. https://doi.org/10.1016/j.ijhydene.2020.06.183.
[44] Choudhuri AR, Gollahalli SR. Combustion characteristics of hydrogen–hydrocarbon hybrid fuels. Int J Hydrogen Energy 2000;25(5):451–62. https://doi.org/10.1016/S0360-3199(99)00027-0.
[45] Wu L, Kobayashi N, Li Z, Huang H, Li J. Emission and heat transfer characteristics of methane–hydrogen hybrid fuel laminar diffusion flame. Int J Hydrogen Energy 2015;40(30):9579–89. https://doi.org/10.1016/j.ijhydene.2015.05.096.
[46] Kumar P, Mishra DP. Experimental investigation of laminar LPG–H2 jet diffusion flame. Int J Hydrogen Energy 2008;33(1):225–31. https://doi.org/10.1016/j.ijhydene.2007.09.023.
[47] Choudhuri AR, Gollahalli SR. Characteristics of hydrogen–hydrocarbon composite fuel turbulent jet flames. Int J Hydrogen Energy 2003;28(4):445–54. https://doi.org/10.1016/S0360-3199(02)00063-0.
[48] Ricou FP, Spalding D. Measurements of entrainment by axisymmetrical turbulent jets. J Fluid Mech 1961;11(1):21–32. https://doi.org/10.1017/S0022112061000834.
[49] Buch R, Hamins A, Konishi K, Mattingly D, Kashiwagi T. Radiative emission fraction of pool fires burning silicone fluids. Combust Flame 1997;108(1):118–26. https://doi.org/10.1016/S0010-2180(96)00098-3.
[50] Langman AS, Nathan GJ, Mi J, Ashman PJ. The influence of geometric nozzle profile on the global properties of a turbulent diffusion flame. Proc Combust Inst 2007;31(1):1599–607. https://doi.org/10.1016/j.proci.2006.07.165.

Please cite this article as: Gee AJ et al., Hydrogen addition to a commercial self-aspirating burner and assessment of a practical burner modification strategy to improve performance, International Journal of Hydrogen Energy, https://doi.org/10.1016/j.ijhydene.2023.06.230

[51] Kuntikana P, Kadoli R, Prabhu S. Investigations on entrainment of surrounding fluid in jet flow in to a cylindrical tube nozzle. In: Innovative solutions in flow measurement and control - oil, water and gas; 2017.
[52] Messaoudani Zl, Rigas F, Binti Hamid MD, Che Hassan CR. Hazards, safety and knowledge gaps on hydrogen transmission via natural gas grid: a critical review. Int J Hydrogen Energy 2016;41(39):17511–25. https://doi.org/10.1016/j.ijhydene.2016.07.171.
[53] Kalantari A, McDonell V. Boundary layer flashback of non-swirling premixed flames: mechanisms, fundamental research, and recent advances. Prog Energy Combust Sci 2017;61:249–92. https://doi.org/10.1016/j.pecs.2017.03.001.
[54] Eichler C, Baumgartner G, Sattelmayer T. Experimental investigation of turbulent boundary layer flashback limits for premixed hydrogen-air flames confined in ducts. J Eng Gas Turbines Power 2011;134(1). https://doi.org/10.1115/1.4004149.
[55] Paul SC, Paul MC. Radiative heat transfer during turbulent combustion process. Int Commun Heat Mass Tran 2010;37(1):1–6. https://doi.org/10.1016/j.icheatmasstransfer.2009.10.005.
[56] Turns SR, Myhr FH, Bandaru RV, Maund ER. Oxides of nitrogen emissions from turbulent jet flames: part II—fuel dilution and partial premixing effects. Combust Flame 1993;93(3):255–69.
[57] Xi Z, Fu Z, Hu X, Sabir SW, Jiang Y. An investigation on flame shape and size for a high-pressure turbulent non-premixed swirl combustion. Energies 2018;11:930. https://doi.org/10.3390/en11040930.
[58] Roper F. The prediction of laminar jet diffusion flame sizes: Part I. Theoretical model. Combust Flame 1977;29:219–26. https://doi.org/10.1016/0010-2180(77)90113-4.
[59] Roper F, Smith C, Cunningham A. The prediction of laminar jet diffusion flame sizes: Part II. Experimental verification. Combust Flame 1977;29:227–34. https://doi.org/10.1016/0010-2180(77)90112-2.
[60] Glassman I, Yetter RA, Glumac NG. Combustion. Academic press; 2014.
[61] Wang Z, Wang S, Whiddon R, Han X, He Y, Cen K. Effect of hydrogen addition on laminar burning velocity of CH4/DME mixtures by heat flux method and kinetic modeling. Fuel 2018;232:729–42. https://doi.org/10.1016/j.fuel.2018.05.146.
[62] Law CK. Combustion physics. Cambridge: Cambridge University Press; 2006.
[63] Chen Y, Kahangamage U, Zhou Q, Leung C. Can hydrogen enriched biogas be used as domestic fuel? - Part I – thermal Characteristics of Blended Biogas/H2 Impinging Flames. Trans Hong Kong Inst Eng 2021;28:60–7. https://doi.org/10.33430/V28N2THIE-2020-0040.
[64] Cellek MS, Pınarbaşı A. Investigations on performance and emission characteristics of an industrial low swirl burner while burning natural gas, methane, hydrogen-enriched natural gas and hydrogen as fuels. Int J Hydrogen Energy 2018;43(2):1194–207. https://doi.org/10.1016/j.ijhydene.2017.05.107.
[65] Guo H, Smallwood GJ, Liu F, Ju Y, Gülder ÖL. The effect of hydrogen addition on flammability limit and NOx emission in ultra-lean counterflow CH4/air premixed flames. Proc Combust Inst 2005;30(1):303–11. https://doi.org/10.1016/j.proci.2004.08.177.
[66] Meloni R, Nassini PC, Andreini A. Model development for the simulation of the hydrogen addition effect onto the NOx emission of an industrial combustor. Fuel 2022;328:125278. https://doi.org/10.1016/j.fuel.2022.125278.
[67] Ma F, Wang Y, Liu H, Li Y, Wang J, Zhao S. Experimental study on thermal efficiency and emission characteristics of a lean burn hydrogen enriched natural gas engine. Int J Hydrogen Energy 2007;32(18):5067–75. https://doi.org/10.1016/j.ijhydene.2007.07.048.
[68] Shudo T, Mizuide T. NOx emission characteristics in rich–lean combustion of hydrogen. JSAE Rev 2002;23(1):9–14. https://doi.org/10.1016/S0389-4304(01)00163-1.
[69] Balicki W, Głowacki P, Szczeciński S, Chachurski R. Aviation – environmental threats. Journal of KONES 2014;21. https://doi.org/10.5604/12314005.1134048.
[70] Andrieu A, Allgaier O, Leyssens G, Schönnenbeck C, Brilhac J-F, Brillard A, Tschamber V. NOx reduction based on N2 dilution in a swirled-stabilized magnesium flame. Fuel 2023;341:127702. https://doi.org/10.1016/j.fuel.2023.127702.
[71] Pignatelli F, Kim H, Subash AA, Liu X, Szasz RZ, Bai XS, Brackmann C, Aldén M, Lörstad D. Pilot impact on turbulent premixed methane/air and hydrogen-enriched methane/air flames in a laboratory-scale gas turbine model combustor. Int J Hydrogen Energy 2022;47(60):25404–17. https://doi.org/10.1016/j.ijhydene.2022.05.282.
[72] Mohammadpour A, Mazaheri K, Alipoor A. Reaction zone characteristics, thermal performance and NOx/N2O emissions analyses of ammonia MILD combustion. Int J Hydrogen Energy 2022;47(48):21013–31. https://doi.org/10.1016/j.ijhydene.2022.04.190.
[73] Moore M. NOx emission control in gas turbines for combined cycle gas turbine plant. Proc Inst Mech Eng A J Power Energy 1997;211(1):43–52. https://doi.org/10.1243/0957650971536980.
[74] Chen R-H, Driscoll JF. Nitric oxide levels of jet diffusion flames: effects of coaxial air and other mixing parameters. Symposium (International) on Combustion 1991;23(1):281–8. https://doi.org/10.1016/S0082-0784(06)80271-7.

Please cite this article as: Gee AJ et al., Hydrogen addition to a commercial self-aspirating burner and assessment of a practical burner modification strategy to improve performance, International Journal of Hydrogen Energy, https://doi.org/10.1016/j.ijhydene.2023.06.230